



ELSEVIER

Contents lists available at ScienceDirect

Building and Environment

journal homepage: www.elsevier.com/locate/buildenv

Performance of Hong Kong's common trees species for outdoor temperature regulation, thermal comfort and energy saving



Tobi Eniolu Morakinyo^{a,*}, Kevin Ka-Lun Lau^a, Chao Ren^{a,b}, Edward Ng^{a,b}

^a Institute of Future Cities, The Chinese University of Hong Kong, New Territories, Hong Kong

^b School of Architecture, The Chinese University of Hong Kong, New Territories, Hong Kong

ARTICLE INFO

Keywords:

Temperature regulation
Energy saving
Thermal comfort
Tree species
ENVI-met

ABSTRACT

Using a validated ENVI-met model, a parametric study was conducted to investigate the thermal and energy saving benefits in a selected neighbourhood with its current greenery coverage ratio (GCR) of 7.2%, compared to the recommended 30%. To provide information for efficient tree species selection, nine scenarios were tested for the case of 30% GCR. In eight of them, only one tree species was used in each case. The trees represent the eight most common species in Hong Kong. The remaining one featured a mix of tree species.

In comparison with the reference case (no trees), results revealed a reduction in maximum temperature of 0.4 °C and 0.5–1.0 °C under the current and 30% GCR situations respectively; and a decrease in average Physiological Equivalent Temperature of 1.6 °C and 3.3–5.0 °C. The area coverage of “Very Hot” thermal sensation reduced from ~60% in the reference case to ~50% with the current GCR and 17–21% with 30% GCR. Lastly, a decrease in cooling energy of 1500 kWh per typical summer day was observed with the current GCR, which increased to ~1900–3000 kWh with 30% GCR, equivalent to 200–450 US\$ savings within the 500 × 500 m² domain. The variations in the estimated benefits between the 30% GCR scenarios reflect the importance of species-specific analysis. Statistical analysis revealed leaf area index was the main driver of the observed benefits, followed by trunk height, tree height and crown diameter. Our findings will encourage city planners and citizens to take actions for urban greening.

1. Introduction

1.1. Background of study

Rapid urbanization and global climate change have resulted in various environmental threats such as heat stress and excessive energy demand [1,2]. During the summer period of most tropical and sub-tropical cities or countries, the air temperature difference between urban and rural environment widens. This is known as the Urban Heat Island (UHI) effect and results in an increase in cooling energy consumption in urban areas [3,4]. In fact, the average Global Energy penalty per unit of surface and degree of UHI intensity was estimated as 0.74 kWh/m²/K while the average total energy load of representative buildings consumed for heating and cooling purposes had increased by 11% between 1970 and 2010 [5]. Moreover, the UHI phenomenon intensifies heatwaves and outdoor thermal discomfort. As previous studies revealed that heat related mortality was higher in urbanized areas compared to their rural counterparts [6–8], concerns were raised about the UHI's adverse effect on human's health.

In response, several previous studies focused on the identification and recommendation of technical measures to mitigate the threats, reduce the demand for cooling energy and enhance a city's livability [9–14]. Of the strategies they proposed— such as modifications of building and surface materials, alteration of urban morphology, insulation of buildings and installation of irrigation systems— urban greenery, especially the planting of trees, was suggested to be the most beneficial and sustainable. Green areas or spaces have the capacity to significantly regulate ambient temperature, improve thermal comfort, save energy in the built environment through shading and evapotranspiration, and perform other ecosystem services [15,16]. Because of these benefits, many metropolitan cities are now gradually incorporating greenery into their urban areas through frameworks such as the Greening Master Plans (GMPs) in Hong Kong [17], Green Building Masterplan of Singapore and Greening Sydney Plan.

While greenery (especially trees) is generally known to provide a range of ecosystems services such as stormwater reduction, air pollution mitigation, noise abatement etc. [16], this study focuses on its functions of temperature regulation, outdoor thermal comfort

* Corresponding author.

E-mail address: tobimorak@cuhk.edu.hk (T.E. Morakinyo).

improvement and cooling energy reduction. These benefits are controlled by ambient micrometeorological conditions and can be suitably modified by trees through three main processes [20]. First, the shading effect: through their foliage, trees attenuate a significant amount of incoming shortwave radiation by either reflection or transmission. Thus, the ground surface temperature, sensible heat gain, ground surface and air temperature, and mean radiant temperature (MRT) below the tree canopy are reduced [21–23]. MRT is a key determinant of human thermal sensation during daytime [24,25], meaning that the level of thermal comfort under tree shade is higher than in an open space [26–28]. Furthermore, trees provide transpirational cooling through water vapor dissipation to the air via their leaf stomata, lowering the temperature of the leaf surfaces and surrounding environment [29]. Lastly, general knowledge suggests that trees cause wind resistance i.e. reduced urban ventilation. However, there are some exceptions, especially when urban morphology and prevailing flow angle are considered. A recent study [30] has shown low impact of trees in high-density areas and vice-versa for low-density settings. Also, this ventilation effect is a function of the prevailing direction with oblique wind flow being more impeded than perpendicular [14].

The aforementioned have a combined effect on the outdoor thermal environment and human thermal comfort, usually objectively determined using thermal indices, such as Physiologically Equivalent Temperature (PET), Standard effective temperature (SET*) and Universal Thermal Climate Index (UTCI). Even though trees might impede wind velocity, their positive role in the other three parameters described earlier help improve thermal comfort in shaded areas [26–28]. In terms of energy saving, buildings shaded by trees are often cooler inside, compared to the unshaded ones. This suggests there is less heat transmission, resulting in a lower demand for and expenditure in cooling energy [31–36]. The result can be explained by the accumulation of cool air under tree covers and the development of that into a three dimensional (3D) urban cool island [37–40]. Thus, urban greening is described as passive coolants or natural air conditioners that save building energy use, especially on hot summer days [37,41–43]. It is important to mention that most previous studies focused on estimating the cooling impact of nearby trees, green-roof and facade greening on building's indoor energy saving [43–47]. Some research was done outdoor but mostly on horizontal scales [48,49] using remote sensing or field measurement techniques. However, the energy saving potential in a 3D (both horizontal and vertical) dimensional manner has not been studied as much [41,50,51].

The magnitude of thermal influence i.e. solar attenuation, MRT reduction, transpiration rate and quantity, temperature regulation and thermal comfort improvement, is another important issue to be considered. It does not only depend on the size and shape of a park or green space, but also varies by tree species and structural characteristics, i.e. leaf density, tree height, crown diameter, coverage ratio and proximity to each other (single or cluster) [52]. Environmental factors (e.g., air temperature, carbon dioxide concentration, soil wetness) and physical configurations of the trees (e.g., tree height, leaves' thickness and colour, and tree trunk and branches' architecture) also play a part [27,53]. Hence, there is a need for research to move past generalization of trees to species-specific analysis of thermal and energy saving benefits for cities and countries around the world.

Therefore, this study, as one of the first to do so, presents a methodology to investigate the ability of different tree species in urban thermal regulation and outdoor energy saving in a 3D domain from numerical simulation results. Specifically, the 3D energy saving potential and thermal regulation performance of eight of Hong Kong's most common tree species for amenity planting in a realistic urban environment were considered. The Urban Climate Map (UCMap) project in Hong Kong [18,19] recommended an urban green coverage ratio of 20–30% in the reduction of urban thermal load, mitigation of the heat island effect and enhancement of the urban climate in general. However, a recent overview of the city's landscape suggests the

greenery goal across the board is yet to be attained, especially in already developed areas. Therefore, this study uses validated ENVI-model simulation to conduct parametric numerical experiments to investigate the thermal and energy saving effects for a selected neighbourhood of 500 m × 500 m in Kowloon Bay, Hong Kong. The current greenery situation of 7.2% GCR is compared to the suggested rate of 30%. Furthermore, species-specific recommendations are devised by testing situations where a single type of tree from the eight most common species in Hong Kong is used in the 30% GCR scenario.

Of the tree species considered, only two are native to Hong Kong or South Asia. The others can also be found in other parts of the world including America, Mexico, South Africa and Australia. This implies that even though the case study here is local, the results can be application to other parts of the world with dominant trees of similar physical configuration. The magnitude of thermal impact, however, may vary due to differences in prevailing weather condition and urban morphology. The results presented here will further inform urban designers, city planners and decision makers on how urban greening recommendations and policies will help improve the local microclimate and thermal regulation of neighborhoods and the city in general. They will be helpful in the enhancement of understanding of the thermal benefits of urban greening, formulation of action plans for greenery conservation and planning, and design for enhanced ecosystem services at site, neighborhood, district, city, and regional scales.

2. Methodology

2.1. Study area

In this study, all field measurements and simulations are aimed at capturing the sub-tropical hot-humid summer climate of Hong Kong, a city known for high-density urban settings. It is situated along the coastline of South East China (22°15'N, 114°10'E) and has an average altitude of 8 m [54]. The city experiences monsoon-influenced sub-tropical climate associated with hot-humid summer months (i.e. May to September) with a typical maximum temperature of 33 °C. In fact, the Hong Kong Observatory [55] has noted a significant increase in the numbers of hot nights and very hot days by 19 and 10 from 1885 to 2015 with a projected increase during the 21st century. To put our study into perspective, we selected a 500 × 500 m² area in Kowloon Bay, Hong Kong (see Fig. 1(a) and (b)) as the main study area for both field measurement and numerical experiments. The neighborhood is in the east of the Kowloon Peninsula and to the north of Hong Kong Island, and classified as a mixed industrial and residential area. This area is composed of buildings (podia included) with heights ranging from 20 to 220 m (according to the data obtained from the Buildings Department, HKSAR). They are oriented in the NW-SE and EW directions and the streets, mainly made of concrete and asphalt, are 15–30 m wide. The area contains some trees, mostly of dense crown *Aleurites moluccana* (candlenut) and sparse crown *Melaleuca quinquenervia* (Paperbark) with an estimated Green Coverage Ratio (GCR) of 7%. In summary, 44% of the area is covered by buildings, 7% by greenery and 49% by other features. The goal of the study is to estimate and compare the thermal and energy saving benefits under the current and recommended GCR with different tree species.

2.1.1. Field measurement

For the purpose of empirical data archiving and model validation, field measurement campaigns were conducted on 23rd August, 15th and 17th October 2016 between 09:00 and 17:00 local time at our study site. Two measurement locations (see Fig. 1 (a) and (b)) were selected: below a *Aleurites moluccana* canopy (tree-shaded) and open-site (unshaded) located on a north-south oriented street canyon. Simultaneous measurements of air temperature (T_a), globe temperature (T_g), relative humidity (RH), and wind speed (v_a) were taken at a 10s sampling interval using one boxed and mounted TESTO480 measuring

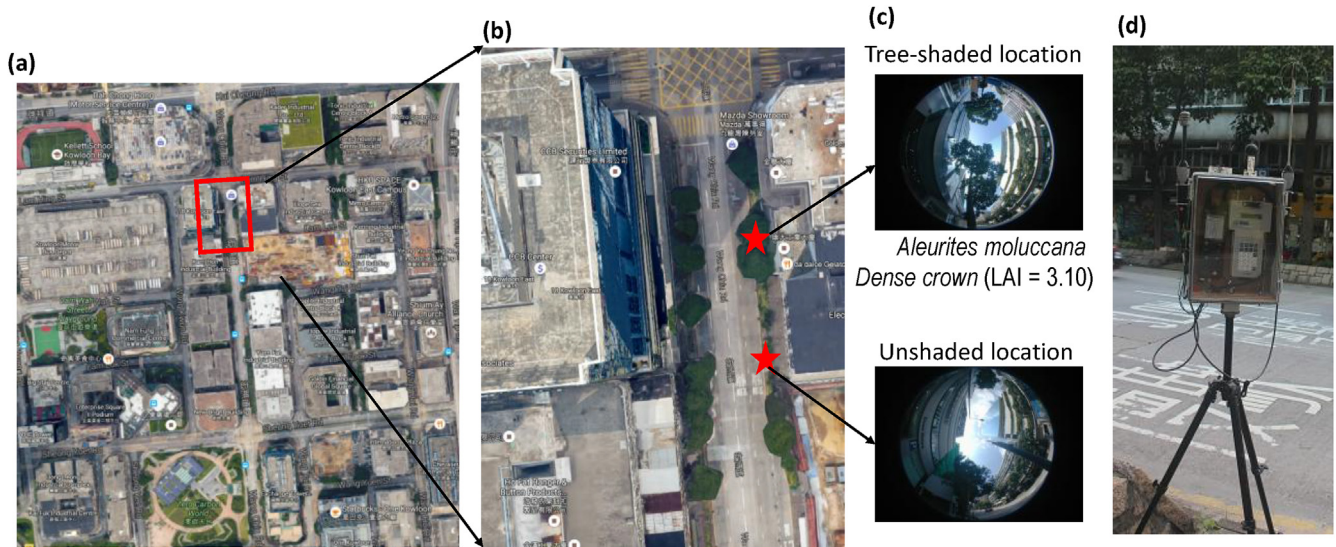


Fig. 1. (a) Satellite view of the Kowloon Bay area of Hong Kong from Google Map; (b) Zoomed-in image of the street-canyon of measurement; red stars indicate measurement points; (c) Fisheye lens images of the measurement locations; and (d) mounted measuring instruments. (For interpretation of the references to colour in this figure legend, the reader is referred to the Web version of this article.)

instruments, each at 1.5 m high. Thereafter, the collected data were adjusted to the hourly scale and the hourly mean radiant temperature (MRT) was derived using Eq. (1) [56]:

$$MRT = \left[(T_g + 273.15)^4 + \frac{1.1 \times 10^8 v_a^{0.6}}{\epsilon D^{0.4}} \times (T_g - T_a) \right]^{0.25} - 273.15 \quad (1)$$

where

MRT is the mean radiant temperature,
 T_g is the globe temperature,
 T_a is the air temperature,
 v_a is the wind speed,
 D is the diameter of the globe (= 30 mm), and
 ϵ is the emissivity of globe (= 0.95)

2.2. ENVI-met model description, setup and initialization

2.2.1. Model description

All simulations in this study were performed with ENVI-met V4 model [57,58] hereafter, ENVI-met. It is a holistic 3D non-hydrostatic model for the simulation of surface-plant-air interactions in a complex environment composed of buildings and surfaces of a diverse configurations of materials and vegetation (trees and/or grasses). Its high spatial (0.5–5 m) and temporal (1–5 s) resolutions enable near-accurate modelling of microclimatic parameters. Plants in ENVI-met are not only seen as static-porous media to solar insolation and wind flow, but also biological and dynamical bodies that interact with the surrounding environment by evapotranspiration and energy absorption. The model is popularly known for its capability to evaluate the effectiveness of urban greenery for heat and heat stress mitigation in cities. Further information on the model, including all embedded equations, documentation and downloads can be found at <http://www.envi-met.info>.

2.2.2. Model setup, parameterization and initialization

As required by the ENVI-met model, an area input file which defines the 3D geometry of the built environment was constructed using Hong Kong Planning Department's 'building footprint' dataset. The buildings were all assumed to be made of concrete while the streets are mainly made of concrete overlaid with asphalt. The area was fitted into 100 × 100 grids at 5 m horizontal resolution equaling a 500 m × 500 m horizontal domain, while the 34 vertical grid with 2 m resolution with

13% telescoping from 30 m height was set to accommodate tall buildings in the domain. In order to minimize errors at the model boundary and improve simulation accuracy, 10 nesting grids were added around the model core area. Furthermore, the model area was rotated 5° away from grid north to align with the geographical north in reality.

2.2.3. Experiment scenarios and introduction to SVF-based tree selection method

Our numerical experiments are made up of ten (10) scenarios grouped into four cases as described below:

- Reference case (Ref.): This case is only composed of building and street elements with no vegetation (see Fig. 2 (a)).
- Base case (BC): This is made up of the existing buildings, surfaces and green cover (see Figs. 1 (a) and Fig. 2(b)). According to our estimation, the current GCR is only at 7% in the selected domain, far below the recommended 30% [59] for UHI abatement in Hong Kong. The dominant trees species in the study area are dense crown *Aleurites moluccana* (candlenut) and sparse crown *Melaleuca quinquenervia* (Paperback). Using Nikon Coolpix 800 with the FC-E8 fisheye lens, hemispherical photographs of one sample of each tree species were captured and processed with Hemisfer software [60] to estimate its leaf area index (LAI) using Miller's [61] Li-Cor LAI-2000 algorithm. The estimated LAI were 3.10 and 2.20 for *Aleurites moluccana* and *Melaleuca quinquenervia* respectively. In ENVI-met, vegetation is modelled using leaf area density (LAD) and not LAI. Therefore, equation (1) [57,62], which shows the relationship between the two, was used to generate the corresponding LAD for each height of the tree given the tree's width and trunk height:

$$LAI = \int_0^h LAD \cdot \Delta z \quad (2)$$

where:

h is the height of the tree (m),
 Δz is vertical grid size (m), and
 LAI is the leaf area index.

LAD is the leaf area density (m^2/m^3)

- Single species, 30% GCR: Here, we assume a situation where the study area adopted the 30% GCR recommendation using a single tree species. Eight (8) tree species were tested in total, one per scenario i.e. T1–T8 (see Table 1 and Fig. 2(c)). By planting trees

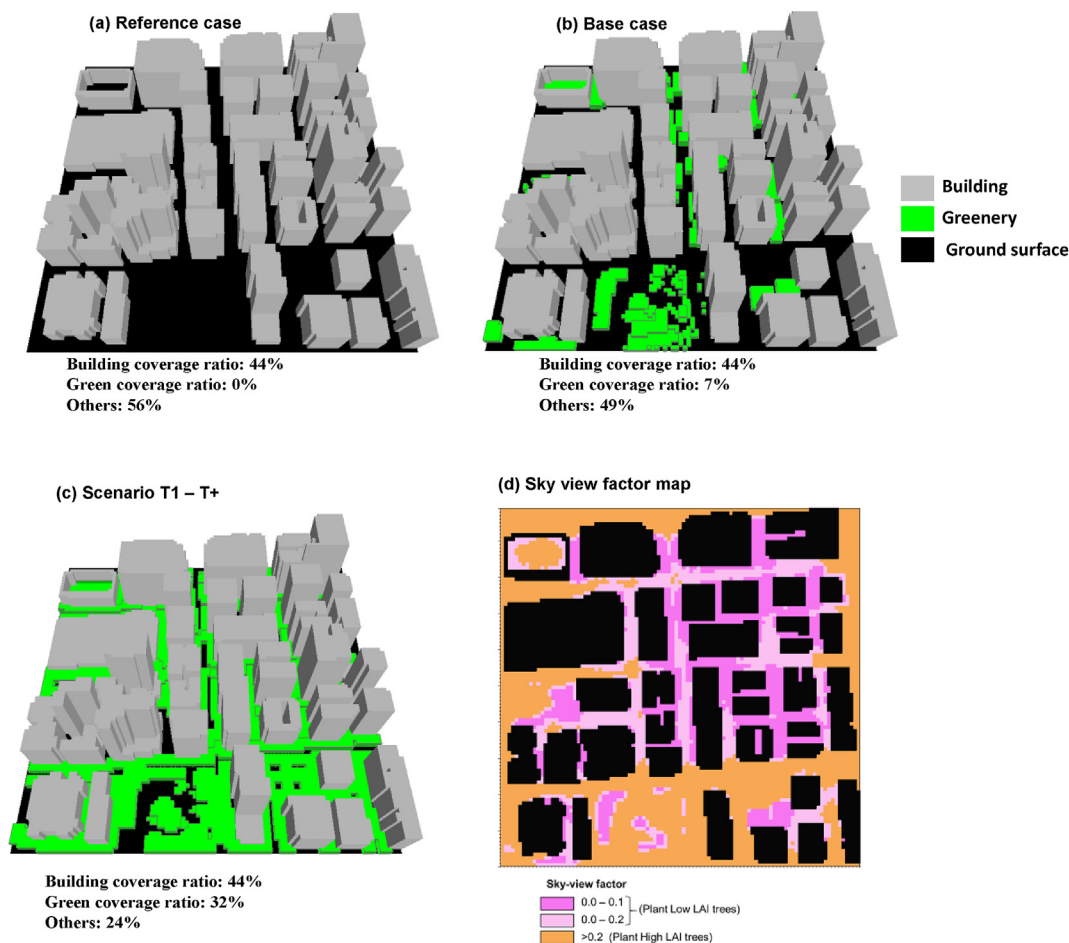


Fig. 2. (a,b,c) Greenery and building coverage extent under various scenarios; (d) sky-view factor map for tree selection decision making.

within and around unshaded car parks, open spaces and on both sides of all street canyons, the GCR of the domain was increased to ~32% [59]. This experiment was aimed at investigating the role of tree configuration in the performance of temperature regulation, energy saving and thermal comfort improvement. The tree species were chosen according to their popularity in amenity planting in Hong Kong [63] and crown width (≤ 8 m). Therefore, they suit the typical and realistic high-density urban setting of Hong Kong. For each species, a representative tree was sampled for the direct measurement of tree height (H_T), trunk height (TH), crown height (CH), and crown width (CW) while the leaf area index (LAI) was estimated using the Hemisfer software [60] based on the captured

hemispherical photographs (Fig. 3). A description of the scenarios and selected trees' physical and morphological configurations are presented in Table 1.

d) SVF-based tree selection case: The scenario (referred to as “T+”) is inspired by the findings from our previous study [63], which suggested the use of sky-view factor or urban density map (see Fig. 2(d)) for tree species selection for urban tree-planting. In the study, we found that shadow-casting effects overrode tree-shading in deep canyons or areas with low SVF. Hence, trees with low foliage density and high trunk height were recommended in such areas and vice-versa for open areas with shallow canyons and high SVF. Therefore, taking reference from the SVF map, T3, *Bombax*

Table 1
Physical configurations of studied tree species and greening scenarios.

Scenario/Tree code	Green Coverage Ratio (%)	Species name	Leaf type	H_T (m)	TH (m)	CH (m)	CW (m)	LAI (m^2/m^2)
Reference case	0	No tree(s)						
Base case	7	<i>Aleurites moluccana</i> and	Evergreen	10	3	7	7	3.10
		<i>Melaleuca quinquenervia</i>	Evergreen	7	2	5	3	2.20
T1	32	<i>Roystonea regia</i>	Evergreen	13	9	4	6	1.1
T2		<i>Casuarina equisetifolia</i>	Evergreen	14	4	10	7	1.52
T3		<i>Bombax malabaricum</i>	Deciduous	6	3	3	7	1.83
T4		<i>Livistona chinensis</i>	Evergreen	11	6	5	6	2.11
T5		<i>Aleurites moluccana</i>	Evergreen	9	3	6	7	2.77
T6		<i>Macaranga tanarius</i>	Evergreen	4	1	3	8	3.02
T7		<i>Melaleuca leucadendron</i>	Evergreen	11	3	8	6	3.42
T8		<i>Bauhinia blakeana</i>	Evergreen	7	2	5	6	3.55
T+		T3 (<i>Bombax malabaricum</i>) and T8 (<i>Bauhinia blakeana</i>)						

H_T : Height of the tree; TH: Trunk height; CH: Crown height; CW: Crown diameter width; LAI: Leaf area index; TM: Transmissivity of downward radiation (%).

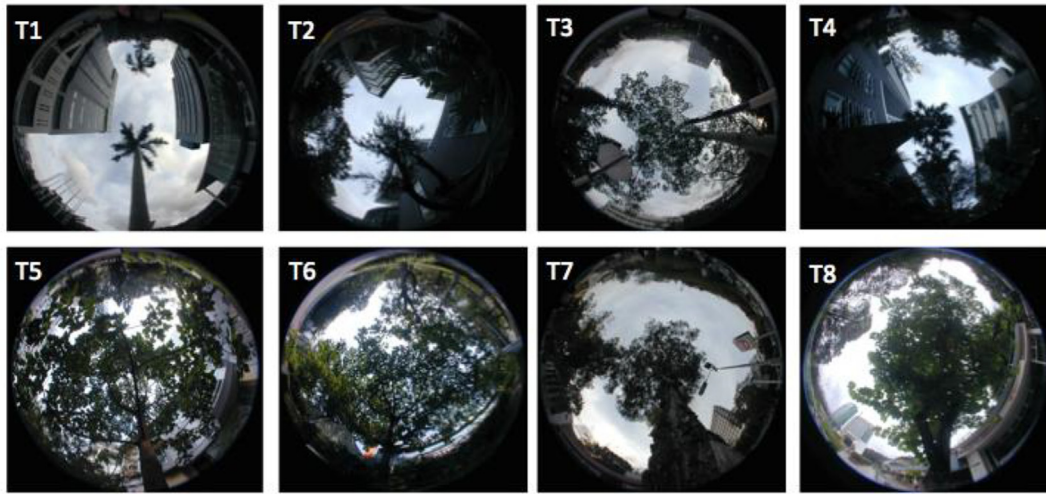


Fig. 3. Hemispherical photographs of the eight (8) selected trees.

malabaricum were planted in areas of $SVF \leq 0.2$ and T8, *Bauhinia blakeana* in $SVF > 0.2$, car park and other open spaces. Earlier results revealed this selection technique would result in thermal benefits (temperature regulation and thermal comfort improvement) similar to a scenario with solely high foliage trees [64].

To mimic a typical summer day in Hong Kong, the model was initialized with the meteorological record of 23rd August, 2016 as shown in Table 1. The hourly air temperature was set to 30 °C, relative humidity at 75%, prevailing wind speed at 2.83 m/s and direction 220°. The data were obtained from the Tseung Kwan O Observatory station, about 5 km east of the study site. Table 2 provides a summary of all the input parameters and values for the validation's simulation exercise. As this study is aimed at testing and estimating the role of trees (species) and coverage, details of vegetation setting and parameterization per scenario are presented below.

2.3. 3D temperature regulation and potential energy saving

To estimate the cooling effects of green coverage, a suitable vertical extent must be assumed. Some previous studies adopted the mean building height [41,51], while others fixed the vertical extent to either pedestrian or tree height [42,50,65]. This indicates a lack of consensus for 3D cooling energy saving estimation. In this study, we propose that the selected height should fulfil two conditions: (1) it is higher than the

tallest tree in the domain; and (2) it shows stability in vertical temperature gradient. Therefore, based on our model setup, we selected the top of the next vertical grid above the tallest tree species under consideration, i.e. 20 m. The daytime mean cumulative 3D temperature reduction $\Delta T_{h,t}$ generated by the green cover from the ground level to height h and within daytime period, t ($t_1 = \text{start time}$ $t_2 = \text{end time}$) was then calculated by the integral Eq. (3):

$$\Delta T_{h,t} = \int_{t_1}^{t_2} \int_0^h [G(h, t) - R(h, t)] dh dt \tag{3}$$

Thereafter, the total energy saving in the 3D domain was estimated based on the $\Delta T_{h,t}$ value. By applying Eq. (4) [41,51] the cooling effect can then be converted to heat reduction i.e. energy saving:

$$\Delta Q_{h,t} = cm\Delta T_{h,t} = c\rho s \int_{t_1}^{t_2} \int_0^h [G(h, t) - R(h, t)] dh dt \tag{4}$$

where:

- $\Delta T_{h,t}$ = Daytime mean cumulative 3D temperature reduction
- $\Delta Q_{h,t}$ = Heat difference between reference and greened scenario from ground level to height h
- $G(h, t)$ = daytime average air temperature at height h in scenario with greenery
- $R(h, t)$ = daytime average air temperature at height h in scenario without greenery
- c = specific heat capacity ($1.0 \times 10^3 \text{ J/kg}^\circ\text{C}$)
- m = mass of air (in kg)
- ρ = air density (1.29 kg/m^3)
- s = size of the green areas (m^2)

2.4. Thermal comfort assessment method

To estimate the effect of GCR and tree species on the study area's thermal comfort, an energy-balance based thermal comfort index, Physiological Equivalent Temperature (PET) was adopted. Derived from the Munich Energy Model for Individuals (MEMI) [66], it is defined as the air temperature at which, in a typical indoor setting (without wind and solar radiation), the heat budget of the human body is balanced with the same core and skin temperature as under the complex outdoor conditions to be assessed [66,67]. The index considers the impact of radiative fluxes on body heat balance in the outdoor environment, making it more acceptable and suitable for assessing outdoor human thermal comfort. For the calculation of PET, simulated

Table 2

Summary of input and test parameters, and the corresponding values for validation simulation of Kowloon Bay area of Hong Kong.

Parameter	Definition	Input value
Meteorological conditions ^a	Initial air temperature (°C)	30
	Relative Humidity (%)	75
	Inflow direction (°)	220
	Wind speed at 10 m (m/s)	2.83
	Soil temperature (°C)	
	Upper, Middle and Deep layer	27.7, 28.9, 29.0
	Solar adjustment	0.9
Buildings'/roads' information	Cloud cover (oktas)	2
	Lateral boundary condition	Open
	Street orientation	NW-SE and EW
	Building Height (m)	20–220
	Street Width (m)	15–30
Tree information	Wall, road and roof albedo	0.3
	See Table 1	

^a Obtained from Hong Kong Observatory (HKO).

Table 3
Thermal sensation classification for Hong Kong.

PET (°C)	Thermal Perception	Physiological stress
< 13	Very cold	Extreme cold stress
13–17	Cold	Strong cold stress
17–21	Cool	Moderate cold stress
21–25	Slightly cool	Slight cold stress
25–29	Neutral	No thermal stress
29–33	Slightly Warm	Slight heat stress
33–37	Warm	Moderate heat stress
37–41	Hot	Strong heat stress
> 41	Very Hot	Extreme heat stress

micro-climate data (air temperature, specific humidity, wind speed and mean radiant temperature) by ENVI-met were imported into an appended software, i.e. BioMet for a standardized person (Age: 35years, Weight: 75 kg, Height: 1.5 m; work metabolism: 80 W of light activity, and 0.9 clo of heat resistance). Afterwards, the calculated values of PET were classified into thermal sensation categories for Hong Kong (see Table 3).

The thermal comfort improvement by greenery was then parameterized, thus:

$$\Delta PET_t = PET_{veg,t} - PET_{ref,t} \tag{5}$$

where

ΔPET_t is the thermal comfort improvement by greenery at a pedestrian height at time t.

$PET_{veg,t}$ is the PET of the study with trees at pedestrian height and at time t.

$PET_{ref,t}$ is the PET of the study without trees at pedestrian height and at time t

3. Result and discussion

3.1. ENVI-met model evaluation

Fig. 4 (a) and (b) show the correlation statistics between the simulated and measured T_a and MRT respectively. Slight discrepancies between the two datasets at both sites were revealed by the quantitative performance statistics tests (see Table 4). They were depicted with three metrics i.e. coefficient of determination (R^2), Root Mean Square Error (RMSE) and Mean Absolute Percentage Error (MAPE). A fairly good correlation of $R^2 = 0.79$ – 0.81 and 0.70 – 0.74 for T_a and MRT respectively was found between the measured values and simulation results (Fig. 4). A relatively low RMSE corresponding to MAPE of 3.7% (for tree-shaded T_a), 5.1% (for unshaded T_a), 7.7% (for tree-shaded MRT) and 13.2% (for unshaded MRT) was found. Previous studies in

Table 4
Quantitative measures of the performance of the ENVI-met model based on measured air temperature, and mean radiant temperature (sample size: 24); R^2 : coefficient of determination, RMSE: root mean square error, MAPE: Mean Absolute Percentage Error.

Parameter	R^2	RMSE(°C)	MAPE (%)
Air temperature			
Tree-shaded	0.81	1.0	3.7
Unshaded	0.79	1.4	5.1
Mean Radiant temperature			
Tree-shaded	0.74	2.2	7.7
Unshaded	0.69	3.9	13.2

Hong Kong and elsewhere also found a strong correlation i.e. $R^2 = 0.79$ – 0.96 and $R^2 = 0.77$ – 0.85 between ENVI-met modelled and measured typical hourly summer T_a [15,22,64,68,69] and MRT [64,70,71] respectively with minimal error.

The observed discrepancies are either due to model limitations or the quality of input data. With respect to the latter, thermal properties of buildings wall, roofs and surfaces were assumed in our model, whereas information by field measurement with proper instruments could probably provide a better result. In terms of model limitation, fixed wind condition and static cloud-free condition were assumed and that may be responsible for the overestimation of incoming solar radiation and other solar-dependent parameters, especially at the unshaded site. Also, the model did not account for anthropogenic heat from vehicles and mechanical cooling systems. Nonetheless, the satisfactory performance statistics obtained from our model evaluation results suggest the ENVI-met model is a reasonably reliable tool for studying plant-surface-atmosphere interaction. It was therefore adopted for the parametric study using the tested and validated setting.

3.2. 3D cooling capacity of greening: comparison of tree species

Considering the entire domain, Fig. 5(a) shows the horizontal (XY) average hourly air temperature variation during the daytime period (09:00–18:00) at pedestrian height (1.5m). The spatial distribution is presented in Fig. 6. The effect of trees (tree species) increased with solar intensity and became more evident in the period of maximum temperature (15:00–16:00), as shown in Fig. 5. In the morning, (09:00–10:00) the cooling effect in terms of temperature difference ($\Delta T_a = T_{a(\text{reference})} - T_{a(\text{green case})}$) was 0.1–0.4 °C, compared to 0.5–1.0 °C during the period of maximum temperature, irrespective of the scenarios. It was also found that a higher GCR resulted in cooler air as supported by previous studies [28,59]. The cooling effect in the base case (7% GCR) was 0.1–0.4 °C irrespective of time, whereas in scenarios with 30% GCR, it ranged from 0.1 to 1.0 °C. Considering the effect of

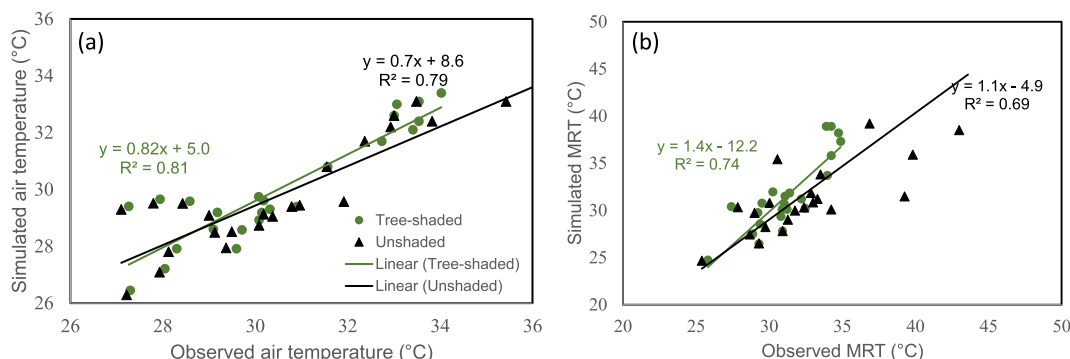


Fig. 4. Relationship between ENVI-met simulated and observed (a) air temperature and (b) mean radiant temperature, MRT at tree-shaded and unshaded location on 23rd August, 15th and 17th October 2016 (09:00–17:00 local time).

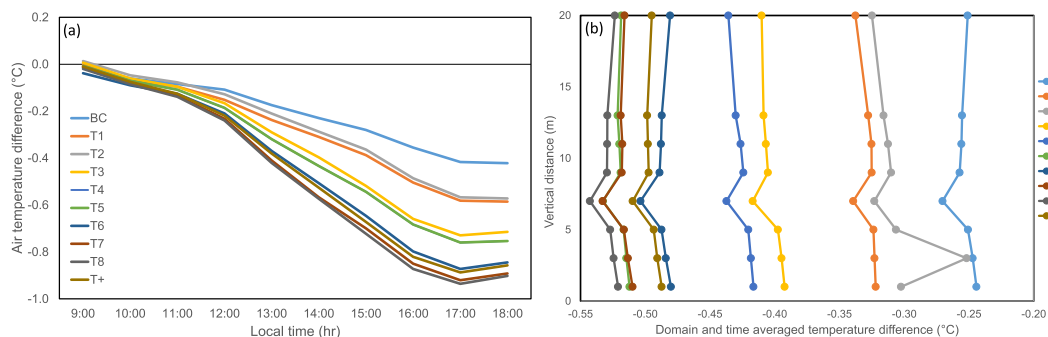


Fig. 5. (a) Hourly variation of domain averaged air temperature at pedestrian height (b) spatio-temporal averaged temperature difference along the vertical distance.

tree species, the maximum ΔT_a observed at 15:00 was 0.5 °C for T1 & T2, 0.7–0.8 °C for T4, T5, T6 and ~1 °C for T7, T8 and T+.

On the vertical scale, the domain and time-averaged vertical air cooling effect of greening is presented in Fig. 5 (b). It shows a similar vertical pattern for all scenarios (except for T2) with similar cooling impact along the vertical distance. However, a cooler zone (by 0.1 °C) was found at about 7 m where the leaves of most of the trees are dominant. It is important to note that the magnitude of cooling varies with GCR and tree species (physical configuration). Four clusters can be observed: Base case, with the least cooling impact across the heights, followed by T1 and T2 (Low LAI trees) of ~0.3 °C, T3 & T4 (moderate LAI trees) of 0.4 °C, and ~0.5 °C for others. In the next section, the

cooling process and the effect of tree configuration parameters (which differentiate each species) are explained.

3.3. Cooling process by trees and effect of species' configuration

This section explains the air cooling process and ventilation impact by tree-shading as observed from our simulation results using the data of 15:00 as an illustration (see Fig. 7). The average cooling effect ranges between 0.4 and 0.5 °C for BC, T1 & T2; 0.7–0.8 °C for T4, T5, T6; and 0.8–1.0 °C for T7, T8 and T+ as shown in Fig. 7(a). The following subsections discuss the factors in the cooling process and ventilation impact.

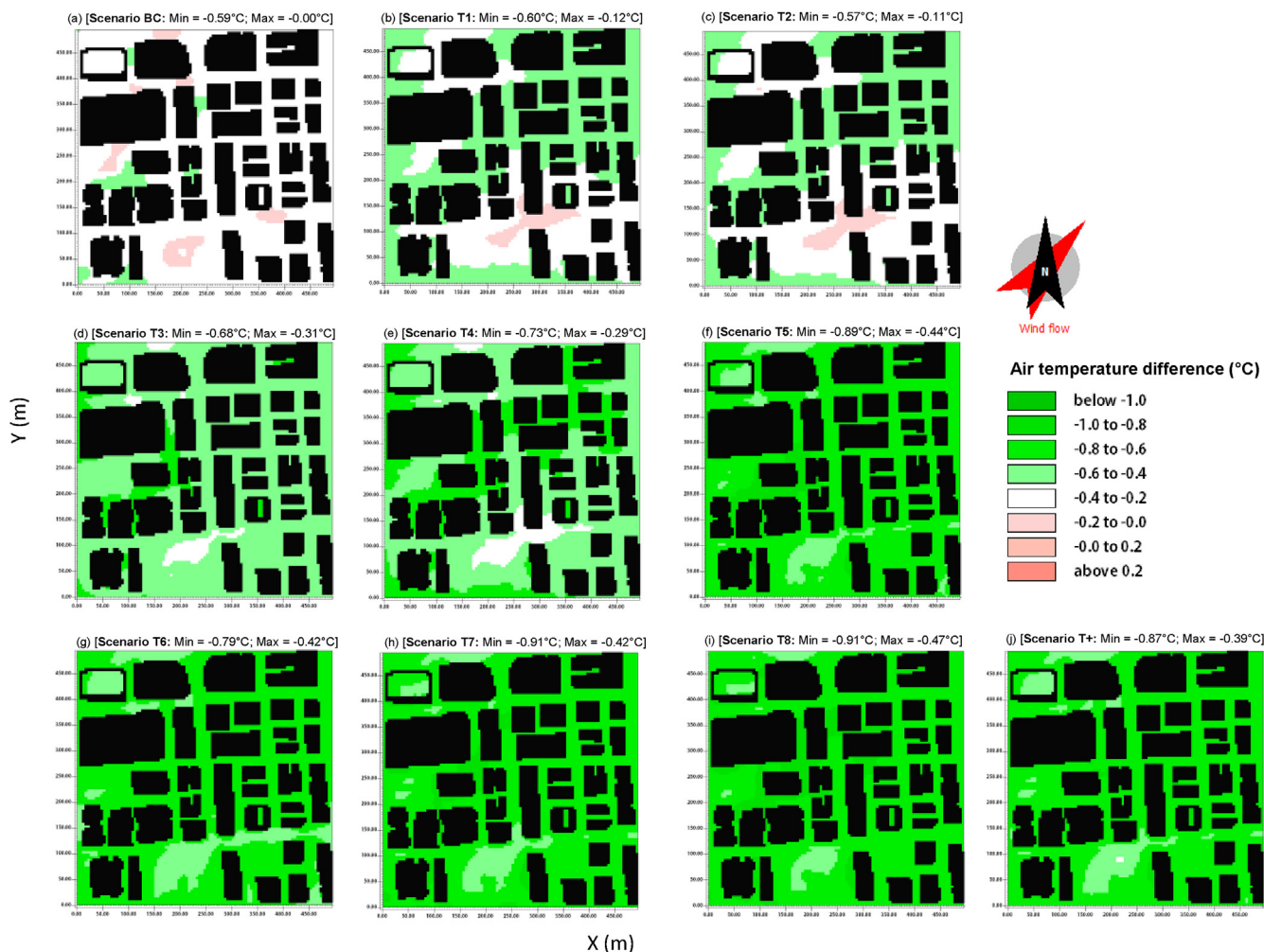


Fig. 6. Cooling effect of tree planting at a pedestrian height at 15:00 under different greened scenarios.

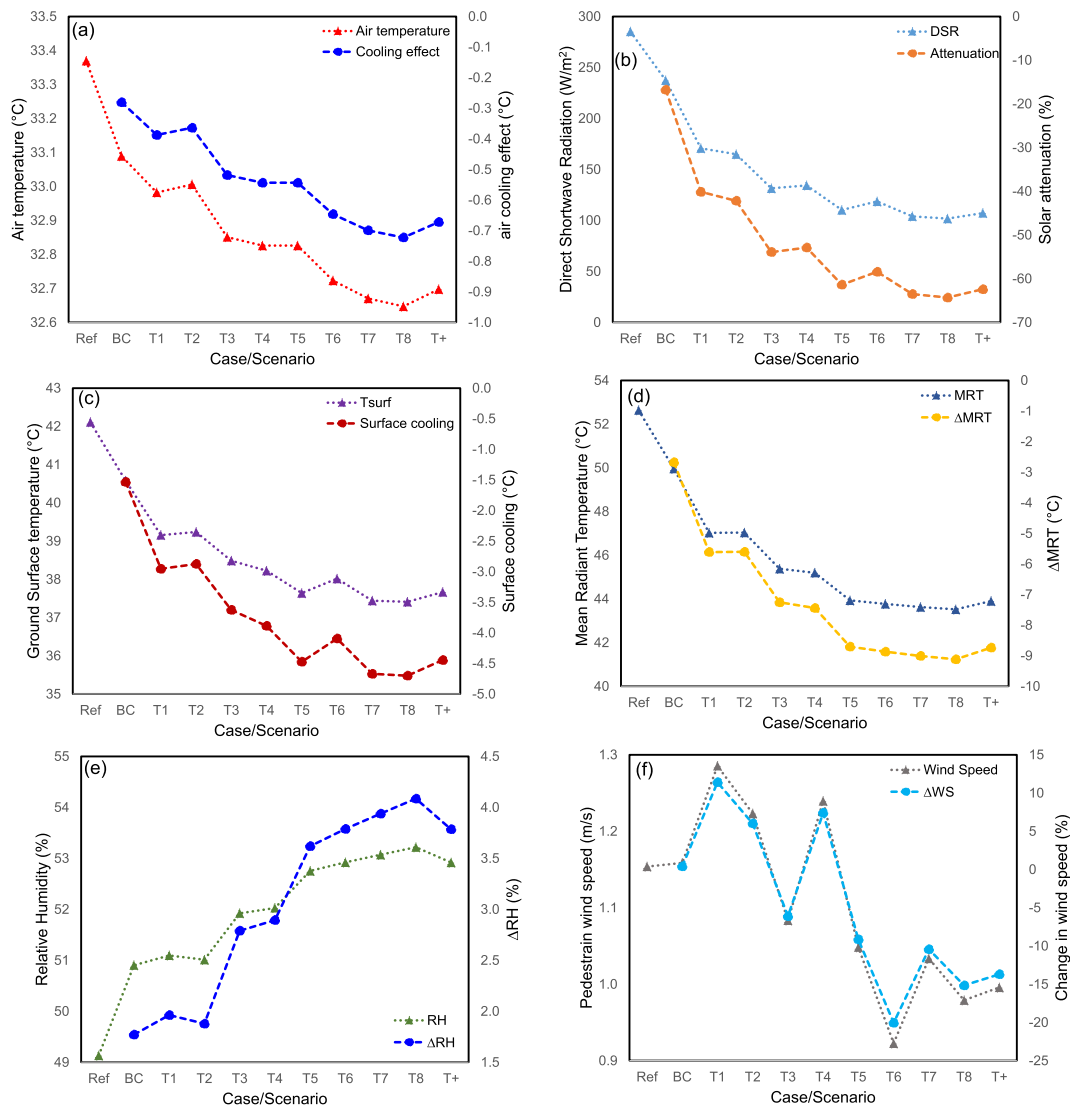


Fig. 7. Effect of vegetation (tree species) and green coverage ratio on microclimate parameters at pedestrian height at 15:00 (as illustrated): mean (a) air temperature; (b) Direct shortwave radiation, DSR; (c) Surface temperature, T_{surf} ; (d) Mean radiant temperature, MRT; (e) Relative Humidity; (f) Wind speed. (For interpretation of the references to colour in this figure legend, the reader is referred to the Web version of this article.)

Table 5
Relationship (R^2) between trees' configuration parameters and meteorological parameters.

Tree configuration/Parameter	LAI	H_T	TH	CH	CW
$\Delta T_a = T_{a(Reference)} - T_{a(Green\ case)}$	+0.91**	-0.39*	-0.44*	0.04	0.01
$\Delta DSR = DSR_{(Reference)} - DSR_{(Green\ case)}$	+0.87***	-0.39*	-0.44*	0.04	0
$\Delta RH = RH_{(Reference)} - RH_{(Green\ case)}$	+0.94***	-0.42*	-0.52**	0.03	0.03
$\Delta WS = WS_{(Reference)} - WS_{(Green\ case)}$	+0.73***	-0.68**	-0.81***	0.06	0.2
$\Delta MRT = MRT_{(Reference)} - MRT_{(Green\ case)}$	+0.92***	-0.44*	-0.54**	0.04	0.01
$\Delta PET = PET_{(Reference)} - PET_{(Green\ case)}$	+0.89***	-0.35*	-0.42**	0.03	0.001
$\Delta Q_{h,t} = Q_{h,t(Reference)} - Q_{h,t(Green\ case)}$	+0.89***	-0.35*	-0.43*	0.04	0.01
Multiple Linear Regression equations				R^2	AR^2
$\Delta T_a = -0.12LAI + 0.014H_T - 0.004TH + 0.044CW + 0CH - 0.68$				0.98**	0.61**
$\Delta DSR = -7.35LAI + 0.671H_T + 0.474TH + 2.429CW + 0CH - 61.1$				0.93*	0.51*
$\Delta RH = 0.99LAI - 0.067H_T + 0.091TH + 0.051CW + 0CH + 0.66$				0.99**	0.63**
$\Delta WS = -7.35LAI + 1.09H_T + 0.609TH - 2.972CW + 0CH - 20.9$				0.96**	0.58**
$\Delta MRT = -1.638LAI + 0.113H_T - 0.152TH - 0.17CW + 0CH - 3.088$				0.97**	0.59**
$\Delta PET = -0.765LAI + 0.045H_T - 0.09TH - 0.039CW + 0CH - 2.109$				0.93*	0.5*
$\Delta Q_{h,t} = -619.2LAI + 35.29H_T - 73.87TH - 42.93CW + 0CH - 920.1$				0.93*	0.5*

***Significant at 99% confidence interval **Significant at 95% confidence interval *Significant at 90% confidence interval.

LAI = Leaf Area Index; H_T = Tree height; TH = Trunk height; CH = Crown Height; CW = Crown width.

T_a = air temperature; RH = Relative Humidity; WS = Wind Speed; MRT = Mean Radiant Temperature; PET = Physiological Equivalent Temperature; $Q_{h,t}$ = 3D energy used up to height h during period; tR^2 = correlation coefficient; AR^2 = Adjusted correlation coefficient; (+) = Positive correlation; and (-) = Negative correlation.

3.3.1. Shading effect

A cause of the observed air cooling is the shading effect. We characterized this by calculating the difference in the average direct shortwave radiation (hereafter, DSR) of the entire study domain, as presented in Fig. 7(b), between the reference and each greenery scenario. In comparison with the reference case, the base case (7% GCR) attenuated 16% of DSR. In the case of the recommended 30% GCR, 40–64% of DSR was attenuated. The variation was dependent on the configuration of the tree species planted, and that was mainly determined by the LAI. A strong correlation ($R^2 = 0.87$) was found between LAI and DSR attenuation (see Table 5). For instance, T1 (*Roystonea regia*) of LAI = 1.1 attenuated 40% of DSR while the T8 (*Bauhinia blakeana*) with the highest LAI of 3.55 attenuated 64%. Trunk height ($R^2 = 0.44$) and tree height ($R^2 = 0.39$) also play a large part in solar attenuation. This implies lower trunk and shorter trees could potentially reduce more solar penetration to the pedestrian level than others. Multiple regression statistics showed $R^2 = 0.93$ and Adjusted $R^2 = 0.61$, indicating a significant contribution of the tested tree configuration variables to the prediction of the solar attenuation. As a result, the average surface temperature of the domain was also reduced by 1.5 °C in the base case scenario. The reduction could be increased to 3.0–4.7 °C if the recommended 30% GCR is followed (see Fig. 7(c)). The magnitude of surface temperature reduction was also dependent on the physical configuration of the planted species and followed a similar pattern to DSR. Please see Table 5 for the corresponding linear regression statistics.

As a consequence of the reduced DSR and surface temperature, the cumulative incident radiative fluxes on pedestrians from all directions lower. The average mean radiant temperature of the greenery compared to the reference scenario can be found in Fig. 7(d). However, the magnitude of this reduction was also dependent on the GCR and physical characteristics of the planted trees (i.e. tree species). Our results revealed a ΔMRT ($\text{MRT}_{\text{greened}} - \text{MRT}_{\text{reference}}$) of 2.7 °C in the base case (7% GCR). In scenarios where the 30% GCR recommendation was followed, the ΔMRT ranged between 5.6 °C and 9.1 °C. The discrepancies were likewise related to the physical configurations of the trees as shown in Table 5. It shows ΔMRT was strongly and positively correlated ($R^2 = 0.92$) to LAI, and partially to trunk and tree height i.e. $R^2 = 0.54$ and 0.44. Specifically, T1 (*Roystonea regia*) and T2 (*Casuarina equisetifolia*), with the least LAI, resulted in the least ΔMRT of 5.6 °C, while trees of highly dense foliage, i.e. T6 (*Macaranga tanarius*), T7 (*Melaleuca leucadendron*) and T8 (*Bauhinia blakeana*), led to the highest difference (~9 °C). When a mix of low and high LAI trees was planted according to the SVF-based selection method i.e. T+, ΔMRT stood at 8.7 °C, similar to using solely trees of extremely high LAI, i.e. T8.

3.3.2. Evaporative cooling

As vegetation in ENVI-met is living organism that interacts with the underlying surface and overlying air, we quantified the evaporative cooling potentials of each greenery scenario by calculating the ΔRH (i.e. $\Delta\text{RH}_{\text{reference case}} - \Delta\text{RH}_{\text{green case}}$). Results in Fig. 7(e) reveal humidity was higher in all scenarios with trees than the reference case. However, the amount of extra moisture was dependent on the coverage ratio and tree configuration. For BC, the increment in RH was 1.8%, while it ranged between 2.0% and 4.1% for scenarios with 30% GCR. The magnitude also depended on the tree configurations (see Table 5). A strong correlation ($R^2 = 0.97$) was found between increased humidity (ΔRH) and reduced air temperature (ΔT_a), establishing the evaporative effect on urban air cooling.

3.4. Vegetation and its configuration effect on ventilation

While it is generally believed that trees weaken wind velocity, the magnitude depends on many factors, such as prevailing wind direction, GCR, the tree species planted and urban configuration of a specific area within the domain. A look at the spatial distribution of ventilation

changes (Fig. 8) revealed that stronger wind reduction was prominent in the windward areas which coincidentally were also of lower sky view factor. In the inner core of the domain, a slightly higher wind speed was observed, possibly due to turbulence generation by the edges of the trees. This observation is consistent with a recent study [30] which found the impact of vegetation was greater at open areas than dense ones in the urban environment. As shown in Fig. 7(f), on average, no significant change was found with the base case (~0.4%) in comparison with the reference case. However, with the recommended 30% GCR, change in wind speed ranged between -15 and [+11]%, indicating the role of species selection in managing ventilation in the urban environment. Again, the variation of the impact was dependent on the trees' configuration (see Table 5). Unlike other parameters, ventilation reduction depended on trunk height ($R^2 = 0.81$) the most, followed by LAI ($R^2 = 0.73$), and then tree height ($R^2 = 0.68$). Tall trees with sparse canopy like T1 (*Roystonea regia*), T2 (*Casuarina equisetifolia*), and T4 (*Livistona chinensis*) gave an average ventilation increment of 11%, 6% and 4%. The highest increment was found in the case of T1 which also has a taller trunk. T6 (*Macaranga tanarius*)—the shortest tree in the selection with very dense foliage—gave the most reduction.

3.5. Effect of greening on thermal comfort: comparison of tree species

In this section, the roles of tree species and green coverage ratio (GCR) in thermal comfort are explored. Thermal comfort was estimated with the PET here, a thermal parameter derived from the mathematical combination of air temperature, wind speed, relative humidity and radiative fluxes (i.e. mean radiant temperature).

The spatial distribution of PET at pedestrian level at 15:00 is shown in Fig. 9. Fig. 10 (a) shows the normal distribution of PET on all non-built up grids in our study domain, while Fig. 10 (b) shows the percentage of area covered by dominant thermal classes per scenario. Generally, the thermal sensation at this time ranged between “Warm” and “Very Hot”. However, the magnitude and spatial coverage of each thermal class varied with different GCR and tree configurations. Fig. 10(a) reveals a shift in the distribution pattern between the reference and other greenery scenarios with the curve skewing to the left as the trees' foliage density increases. The mean values of PET were 41.7 °C (Reference case), 40.2 °C (Base case), 38.5 °C (T1), 38.5 °C (T2), 37.9 °C (T3), 37.6 °C (T4) and 37.0–37.2 °C (T5 to T+). This suggests a reduction of 1.5 °C with the current greenery coverage. It could be improved to 3.2–4.2 °C on average if the 30% GCR recommendation was followed, enhancing the level of thermal comfort by at least one thermal class.

To understand the transformation or conversion from one thermal class to another in each scenario, Fig. 10(b) is presented. It shows the area coverage (in %) per thermal class for all scenarios under consideration. It is interesting to note that without greenery (Reference case), ~60% of the unbuilt grid in the domain had a PET > 41 °C (i.e. “Very Hot”). It was reduced to ~50% in the Base Case (7% GCR). With 30% GCR, i.e. other greenery scenarios, the “Very Hot” class was drastically reduced to 17–22%. Another interesting observation is the transformation of the “Very Hot” class to either “Hot” or “Warm” based on the coverage of these classes. More of the “Very Hot” grids were transformed to “Hot” in the scenarios with trees of lower foliage density (T1, T2, T3 and T4) while more transformed from “Very Hot” to “Warm” with denser foliage trees. This shows that denser foliage trees could potentially improve thermal comfort by up to two thermal classes. In fact, with these trees, slightly warm condition was found between 0.2 and 1% of the domain. Another interesting finding is how close the thermal comfort conditions in the T+ scenario—composed of a mix of high and low LAI trees (based on the SVF-based selection technique)—were to T8, the supposedly most beneficial scenario. This can be observed in Fig. 10 (a) and (b). It indicates the opportunity or potential of this method for appropriate tree selection in urban

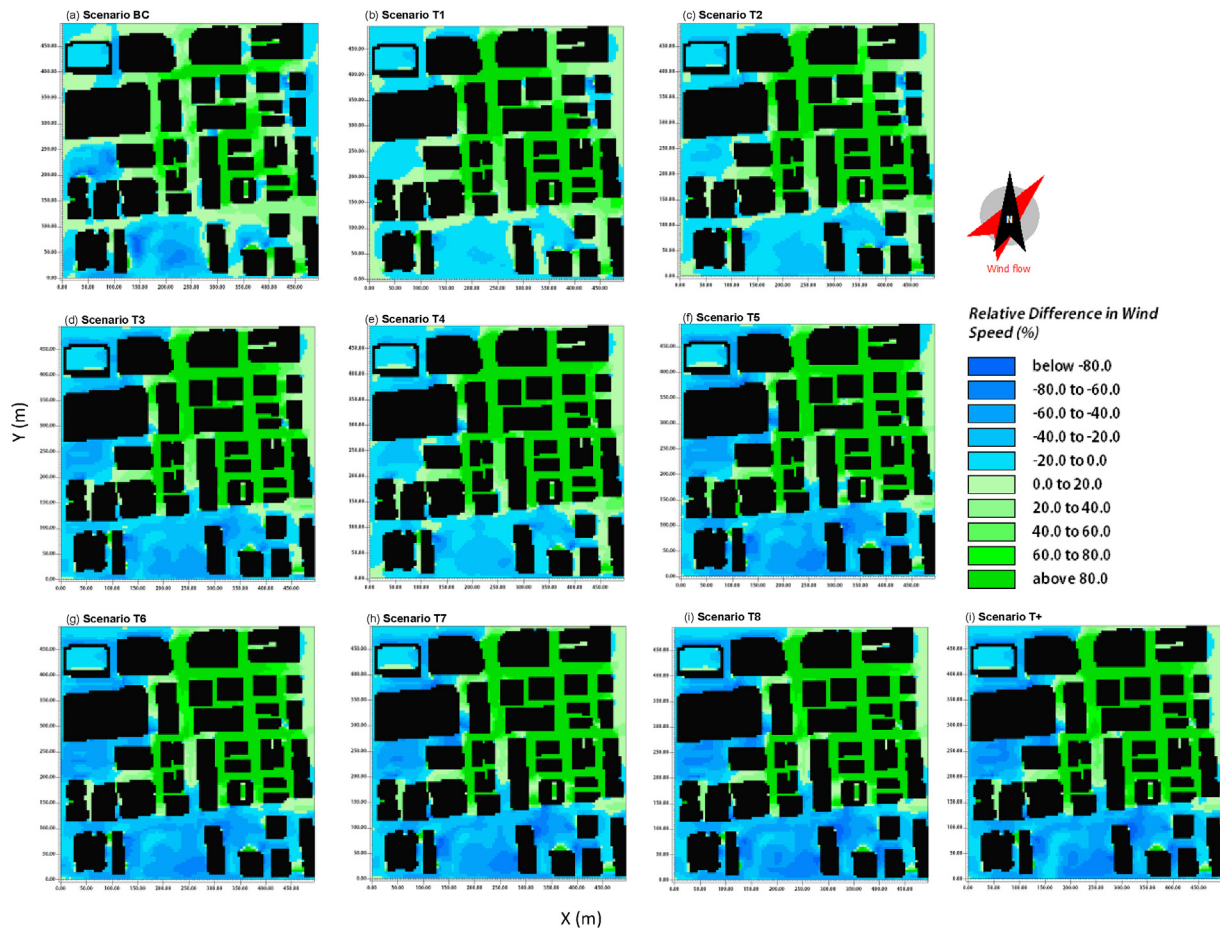


Fig. 8. Influence of tree species and green coverage at pedestrian level ventilation at 15:00. (For interpretation of the references to colour in this figure legend, the reader is referred to the Web version of this article.)

planning. With this method, the species of trees in an urban area can be diversified, while providing the expected thermal benefits.

3.6. Energy saving potential of greening: comparison of tree species

To estimate the energy saving benefits from the cooling effect in our study domain on a typical summer day, Eqs. (3) and (4) were adopted with the vertical height set as 20 m—the next grid above the tallest experimented tree species and where stability in the vertical cooling effect had been actualized. Thus, Eq. (3) can be re-written as:

$$\Delta T_{30, \text{daytime}} = \int_{09:00}^{18:00} \int_0^{20} [G(h, t) - R(h, t)] dh dt \quad (6)$$

Thus, Eq. (6) means the 3D mean cumulative cooling effect of vegetation during the daytime period $t = 09:00\text{--}18:00$ and across different vertical levels, eight in this study. Results of this calculation are presented in Fig. 11(a). It reveals a cumulative daily mean temperature reduction of 5.3°C with the current greenery (7%), improved to $7\text{--}11^\circ\text{C}$ in other scenarios when the 30% GCR recommendation is adopted. Again, the discrepancy is due to the physical characteristics of each tree mostly driven by LAI, tree height and trunk height, in that order (see Table 5). Transforming Eq. (6), the total energy saving over the entire 3D domain from the vegetation's cooling effect was estimated using Eq. (7).

$$\Delta Q_{20, \text{daytime}} = cm\Delta T_{20, \text{daytime}} = c\rho s \int_{09:00}^{18:00} \int_0^{20} [G(h, t) - R(h, t)] dh dt \quad (7)$$

Results presented in Fig. 11(b) reveal cooling energy savings of

about 2 W/m^2 with the Base Case (7% GCR) and $2.5\text{--}8\text{ W/m}^2$ for T1–T8 and T+. In similar studies of university campuses in China [41] and Singapore [72], 5.2 W/m^2 and 5 W/m^2 were estimated for a total green area of 0.08 km^2 (30% GCR) and 0.2 km^2 , respectively. The difference may be due to the morphological properties of the trees in the respective domain which was not considered in the studies.

The cooling effect translates to 1526 kWh and 1992–6348 kWh energy saving during the daytime of a typical summer day for Base Case (7% GCR) and others (30% GCR, T1–T8 and T+) (see Fig. 11(b)). Assuming a room-scale air conditioner has a cooling capacity of $2.8 \times 10^3\text{ W}$ [51], tree planting in the base case would equal 55 air conditioners and a financial saving of $\sim\text{US}\$215$ [1 kWh = 1.11 HK\$; 1 US\$ = 7.825 HK\$] per typical summer day in a $500 \times 500\text{ m}^2$ domain. In the cases of the recommended 30% GCR with T1, T2, T3, T4, T5, T6, T7, T8 and T+, the cooling capacity would equal 71, 67, 87, 92, 112, 104, 111, 113, and 113 air conditioners and a cost reduction of US\$216, US\$282, US\$266, US\$347, US\$366, US\$443, US\$415, US\$442, US\$450 and US\$450, respectively.

4. Key findings, recommendations and conclusion

This study employed a validated ENVI-met model to simulate the microclimate of a $500 \times 500\text{ m}^2$ neighborhood in Kowloon Bay, Hong Kong. The aim was to investigate and quantify the thermal benefits (temperature regulation and thermal comfort improvement) and energy saving potential of the current greenery situation of 7% GCR, compared to the recommendation of 30% GCR by the Hong Kong UCMAP. For the 30% GCR case, eight different trees species were investigated to understand the relationship between trees' physical configurations and

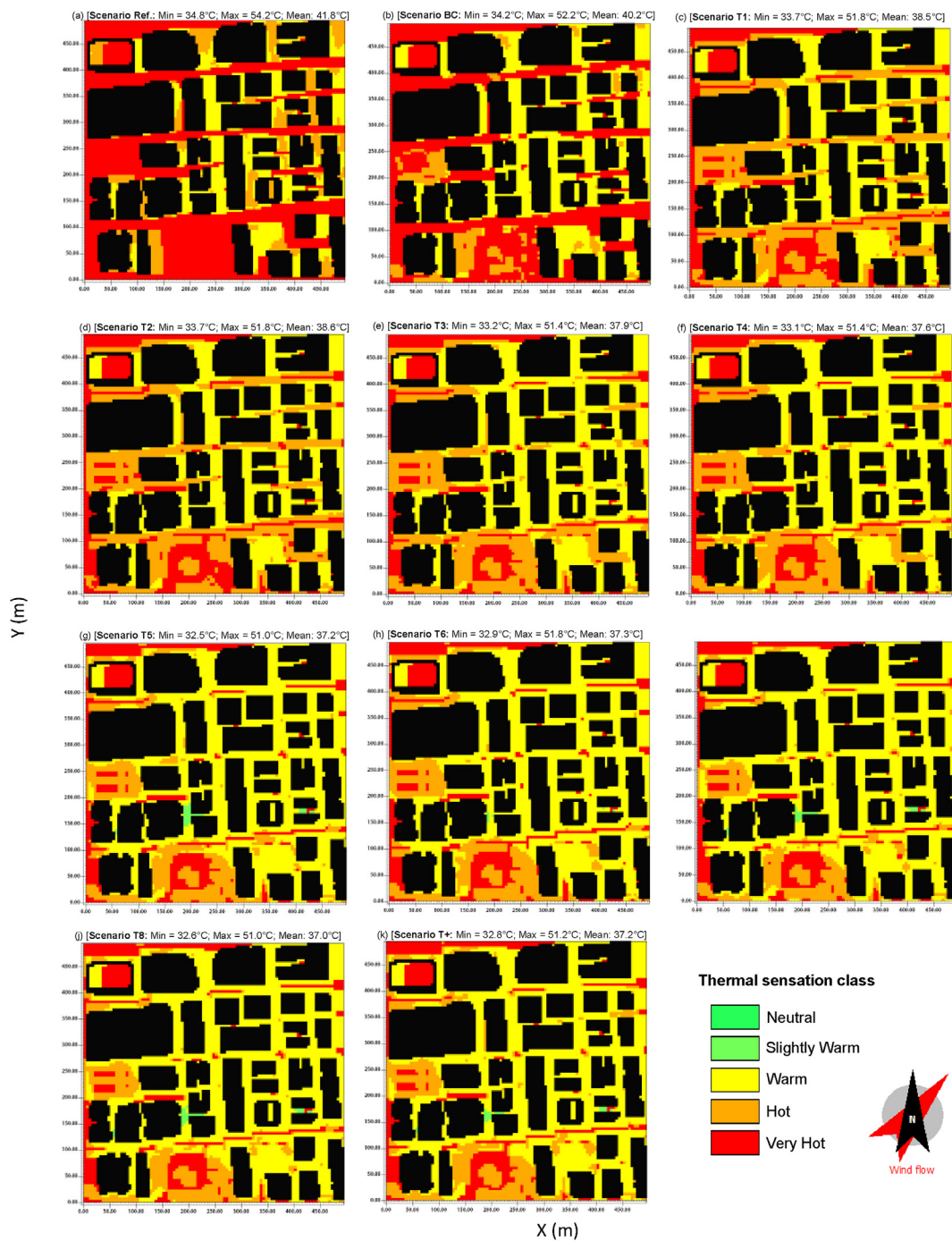


Fig. 9. Influence of tree species and green coverage on pedestrian level PET at 15:00. (For interpretation of the references to colour in this figure legend, the reader is referred to the Web version of this article.)

thermal benefits. The key findings include:

1. The maximum temperature reduction at 15:00 was 0.4 °C and 0.5–0.9 °C with the current and 30% GCR scenarios respectively. It indicates that the magnitude of the cooling effect increases with the percentage of green coverage, similar to the conclusion of other studies in the past [28,48,59].
2. Greenery reduces temperature in a 3D manner (horizontally and vertically at the height of 20 m). The cumulative reduction in the case with 7% GCR was 5.3 °C. It rose to 7–11 °C in the scenarios with 30% GCR.
3. In terms of thermal comfort, the area classified as “Very Hot”

4. Using simple energy equation, a cooling energy saving of 1500 kWh was observed with the current GCR, and it increased to ~1900–3000 kWh per typical summer day with 30% GCR. The latter is equivalent to savings of 200–450US\$ within the 500 × 500 m² domain.
5. Variations of estimated benefits between scenarios with 30% GCR emphasizes the role of tree species (i.e. morphological configuration). Statistical analysis results revealed that the leaf area index was the main driver of the observed thermal and energy-saving benefits, followed by trunk height, tree height and crown diameter.

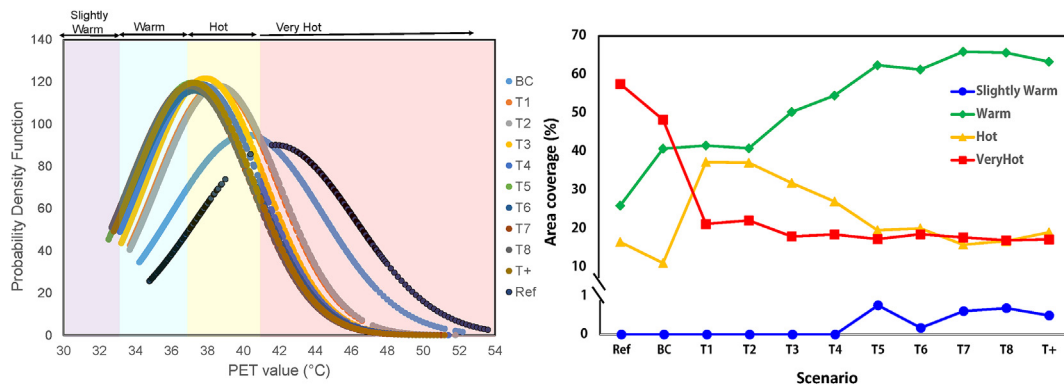


Fig. 10. (a) Probability density distribution of PET values for all scenarios (b) Area coverage of thermal classes in different scenarios (i.e. tree species and green coverage) on at pedestrian level and at 15:00. (For interpretation of the references to colour in this figure legend, the reader is referred to the Web version of this article.)

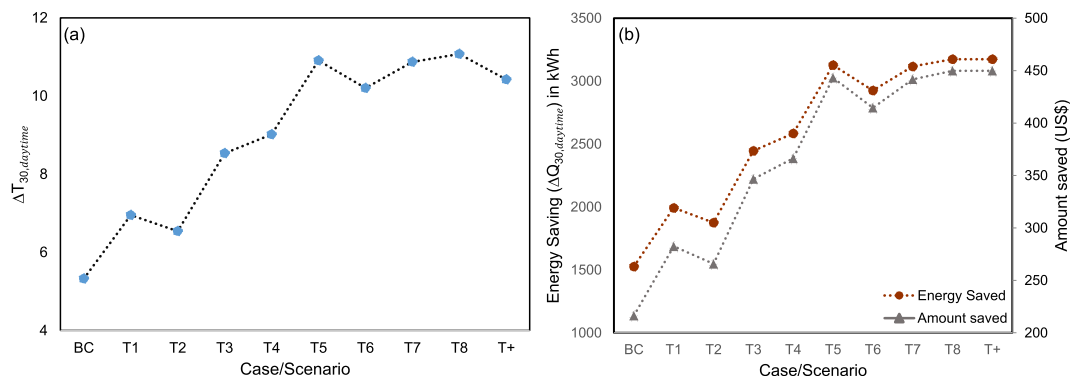


Fig. 11. Effect of vegetation (tree species) and green coverage ratio on (a) daytime 3D cumulative temperature reduction and (b) energy and cost saving. (For interpretation of the references to colour in this figure legend, the reader is referred to the Web version of this article.)

The order of importance for thermal benefits (i.e. temperature regulation, thermal comfort improvement) and energy saving is foliage density, trunk height and tree height. However, for ventilation impact, trunk height has a stronger effect than foliage density and tree height. In any case, the contribution of crown width and height is more or less negligible, especially at the neighbourhood scale.

Therefore, we recommend and encourage a downscaling of the existing Green Master Plan (GMP) from a city/district scale to the community and household levels. Such community engagement, regulated or coordinated by a designated government department, could accelerate the progress of city-scale urban reforestation. Furthermore, as the choice of tree species is crucial for thermal benefits, the urban density (or sky-view factor) map could help in planting the right species at the right place. Specifically, dense foliage trees of an average height such as *Bauhinia blakeana* (T5), *Macaranga tanarius* (T6) and *Aleurites moluccana* (T8) and other similar tree species are suggested for high sky-view factors areas or location e.g. shallow street canyon and other open spaces. On the other hand, sparse foliage tall trees such as *Casuarina equisetifolia* (T2), *Bombax malabaricum* (T3) and others of similar configurations are recommended for low sky-view factors areas such as deep canyons. This technique could effectivity and efficiently aid tree selection for multiple ecosystem services of trees. In fact, the proposed tree species in the current Greening Master Plan (GMP) could be updated based on this approach of urban density (e.g. sky-view factor) mapping.

It important to mention that this study has some limitations related to the adopted ENVI-met model: Firstly, all building facades and roofs have similar thermal properties as a single wall material was adopted, which is not the case in reality. Also, wind flow and cloud condition are kept constant throughout the simulation, contrary to the real

atmosphere. All these factors may affect our estimations of the thermal and energy-saving benefits. Apart from the limitation from the model, we also did not consider some other physical or morphological parameters of trees, such as leaf shape, texture and colour, which have been found to also contribute to the cooling magnitude of trees [73]. Despite these, our results have profoundly confirmed that trees are natural air conditioners through their shading and evapotranspiration cooling capacities. We extended previous works on the subject by presenting species-specific thermal benefits and energy saving potentials of common tree species in Hong Kong. This study is expected to inform policy-makers, community leaders, practitioners and other stakeholders on the benefits of proposed 30% green coverage ratio. Also, our findings provide enhanced knowledge for the planning and design of green spaces, and protection for the environmental quality at both the neighborhood and regional scales.

Acknowledgement

This study was supported by the General Research Fund from the Research Grants Council of Hong Kong (grant numbers: 14629516 & 14611015) and the “Vice-Chancellor’s Discretionary Fund” of the Chinese University of Hong Kong. Special thanks to Dr. Ling Kong for her support in gathering the tree dataset used in this study. Our appreciation also goes to Miss Ada Lee for editing and proof-reading this manuscript.

References

[1] G. Zittis, P. Hadjinicolaou, J. Lelieveld, Projected changes of heat wave characteristics in the Eastern Mediterranean and the Middle East, Int. Conf. Adapt. (2014) 1–12, <http://dx.doi.org/10.1007/s10113-014-0753-2>.
 [2] T. Kjellstrom, I. Holmer, B. Lemke, Workplace heat stress, health and productivity – an increasing challenge for low and middle-income countries during climate

- change, *Glob. Health Action* 2 (2009) 1–6, <http://dx.doi.org/10.3402/gha.v2i0.2047>.
- [3] V. Costanzo, G. Evola, L. Marletta, Energy savings in buildings or UHI mitigation? Comparison between green roofs and cool roofs, *Energy Build.* 114 (2016) 247–255, <http://dx.doi.org/10.1016/j.enbuild.2015.04.053>.
- [4] L. Kleerekoper, M. Van Esch, T.B. Salcedo, How to make a city climate-proof, addressing the urban heat island effect, *Resour. Conserv. Recycl.* 64 (2012) 30–38, <http://dx.doi.org/10.1016/j.resconrec.2011.06.004>.
- [5] M. Santamouris, On the energy impact of urban heat island and global warming on buildings, *Energy Build.* 82 (2014) 100–113, <http://dx.doi.org/10.1016/j.enbuild.2014.07.022>.
- [6] J. Tan, Y. Zheng, X. Tang, C. Guo, L. Li, G. Song, X. Zhen, D. Yuan, A.J. Kalkstein, F. Li, H. Chen, The urban heat island and its impact on heat waves and human health in Shanghai, *Int. J. Biometeorol.* 54 (2010) 75–84, <http://dx.doi.org/10.1007/s00484-009-0256-x>.
- [7] W. Yi, A.P.C. Chan, Effects of Temperature on Mortality in Hong Kong: a Time Series Analysis, (2015), pp. 927–936, <http://dx.doi.org/10.1007/s00484-014-0895-4>.
- [8] S.A. Lowe, An energy and mortality impact assessment of the urban heat island in the US, *Environ. Impact Assess. Rev.* 56 (2016) 139–144, <http://dx.doi.org/10.1016/j.eiar.2015.10.004>.
- [9] M. Santamouris, Cooling the cities - a review of reflective and green roof mitigation technologies to fight heat island and improve comfort in urban environments, *Sol. Energy* 103 (2014) 682–703, <http://dx.doi.org/10.1016/j.solener.2012.07.003>.
- [10] M. Santamouris, A. Synnefa, T. Karlessi, Using advanced cool materials in the urban built environment to mitigate heat islands and improve thermal comfort conditions, *Sol. Energy* 85 (2011) 3085–3102, <http://dx.doi.org/10.1016/j.solener.2010.12.023>.
- [11] S. Lee, Y. Ryu, C. Jiang, Urban heat mitigation by roof surface materials during the East Asian summer monsoon, *Environ. Res. Lett.* 10 (2015) 124012, <http://dx.doi.org/10.1088/1748-9326/10/12/124012>.
- [12] S. Gillner, J. Vogt, A. Tharang, S. Dettmann, A. Roloff, Role of street trees in mitigating effects of heat and drought at highly sealed urban sites, *Landsc. Urban Plann.* 143 (2015) 33–42, <http://dx.doi.org/10.1016/j.landurbplan.2015.06.005>.
- [13] K.J. An, Y.F. Lam, S. Hao, T.E. Morakinyo, H. Furumai, Multi-purpose rainwater harvesting for water resource recovery and the cooling effect, *Water Res.* 86 (2015) 116–121, <http://dx.doi.org/10.1016/j.watres.2015.07.040>.
- [14] T.E. Morakinyo, Y.F. Lam, Simulation study on the impact of tree-configuration, planting pattern and wind condition on street-canyon's micro-climate and thermal comfort, *Build. Environ.* 103 (2016) 262–275, <http://dx.doi.org/10.1016/j.buildenv.2016.04.025>.
- [15] N. Müller, W. Kuttler, A.-B. Barlag, Counteracting urban climate change: adaptation measures and their effect on the thermal comfort, *Theor. Appl. Climatol.* 115 (2013) 243–257, <http://dx.doi.org/10.1007/s00704-013-0890-4>.
- [16] Y. Wang, F. Bakker, R. De Groot, H. Wörtche, Effect of ecosystem services provided by urban green infrastructure on indoor environment: a literature review, *Build. Environ.* 77 (2014) 88–100, <http://dx.doi.org/10.1016/j.buildenv.2014.03.021>.
- [17] HKCEDD, *Greening Master Plan, third ed.*, (2012).
- [18] D. Plan, Urban climatic map and standards for wind environment feasibility study, *Methodol. Find. User's Wind Conf. Lev. Surv.* (2008) 518.
- [19] E. Ng, C. Ren, *The Urban Climatic Map: a Methodology for Sustainable Urban Planning*, Routledge, 2015.
- [20] L. Kong, K.K.-L. Lau, C. Yuan, Y. Chen, Y. Xu, C. Ren, E. Ng, Regulation of outdoor thermal comfort by trees in Hong Kong, *Sustain. Cities Soc.* 31 (2017) 12–25, <http://dx.doi.org/10.1016/j.scs.2017.01.018>.
- [21] D. Armon, P. Stringer, A.R. Ennos, The effect of tree shade and grass on surface and globe temperatures in an urban area, *Urban For. Urban Green.* 11 (2012) 245–255, <http://dx.doi.org/10.1016/j.ufug.2012.05.002>.
- [22] Z. Tan, K.K.L. Lau, E. Ng, Planning strategies for roadside tree planting and outdoor comfort enhancement in subtropical high-density urban areas, *Build. Environ.* 120 (2017) 93–109, <http://dx.doi.org/10.1016/j.buildenv.2017.05.017>.
- [23] S. Sun, X. Xu, Z. Lao, W. Liu, Z. Li, E. Higuera García, L. He, J. Zhu, Evaluating the impact of urban green space and landscape design parameters on thermal comfort in hot summer by numerical simulation, *Build. Environ.* 123 (2017) 277–288, <http://dx.doi.org/10.1016/j.buildenv.2017.07.010>.
- [24] A. Matzarakis, F. Rutz, H. Mayer, Modelling radiation fluxes in simple and complex environments: basics of the RayMan model, *Int. J. Biometeorol.* 54 (2010) 131–139, <http://dx.doi.org/10.1007/s00484-009-0261-0>.
- [25] A. Lai, M. Maing, E. Ng, Observational studies of mean radiant temperature across different outdoor spaces under shaded conditions in densely built environment, *Build. Environ.* 114 (2017) 397–409, <http://dx.doi.org/10.1016/j.buildenv.2016.12.034>.
- [26] M. Fahmy, S. Sharples, On the development of an urban passive thermal comfort system in Cairo, Egypt, *Build. Environ.* 44 (2009) 1907–1916, <http://dx.doi.org/10.1016/j.buildenv.2009.01.010>.
- [27] L.V. de Abreu-Harbach, L.C. Labaki, A. Matzarakis, Effect of tree planting design and tree species on human thermal comfort in the tropics, *Landsc. Urban Plann.* 138 (2015) 99–109, <http://dx.doi.org/10.1016/j.landurbplan.2015.02.008>.
- [28] T. Zölch, J. Maderspacher, C. Wamsler, S. Pauleit, Using green infrastructure for urban climate-proofing: an evaluation of heat mitigation measures at the micro-scale, *Urban For. Urban Green.* 20 (2016) 305–316, <http://dx.doi.org/10.1016/j.ufug.2016.09.011>.
- [29] T.R. Oke, J.M. Crowther, K.G. McNaughton, J.L. Monteith, B. Gardiner, The micrometeorology of the urban forest [and discussion], *Philos. Trans. R. Soc. London B Biol. Sci.* 324 (1989) 335–349.
- [30] C. Yuan, L. Norford, E. Ng, A semi-empirical model for the effect of trees on the urban wind environment, *Landsc. Urban Plann.* 168 (2017) 84–93, <http://dx.doi.org/10.1016/j.landurbplan.2017.09.029>.
- [31] C. Cartalis, A. Synodinou, M. Proedrou, A. Tsangrassoulis, M. Santamouris, Modifications in energy demand in urban areas as a result of climate changes: an assessment for the southeast Mediterranean region, *Energy Convers. Manag.* 42 (2001) 1647–1656, [http://dx.doi.org/10.1016/S0196-8904\(00\)00156-4](http://dx.doi.org/10.1016/S0196-8904(00)00156-4).
- [32] A. Matzarakis, C. Balafoutis, Heating degree-days over Greece as an index of energy consumption, *Int. J. Climatol.* 24 (2004) 1817–1828, <http://dx.doi.org/10.1002/joc.1107>.
- [33] J.C. Lam, C.L. Tsang, D.H.W. Li, Long term ambient temperature analysis and energy use implications in Hong Kong, *Energy Convers. Manag.* 45 (2004) 315–327, [http://dx.doi.org/10.1016/S0196-8904\(03\)00162-6](http://dx.doi.org/10.1016/S0196-8904(03)00162-6).
- [34] M. Christenson, H. Manz, D. Gyalistras, Climate warming impact on degree-days and building energy demand in Switzerland, *Energy Convers. Manag.* 47 (2006) 671–686, <http://dx.doi.org/10.1016/j.enconman.2005.06.009>.
- [35] G. Franco, A.H. Stanstad, Climate change and electricity demand in California, *Clim. Change* 87 (2008) 139–151, <http://dx.doi.org/10.1007/s10584-007-9364-y>.
- [36] O. Guerra Santin, L. Itard, H. Visscher, The effect of occupancy and building characteristics on energy use for space and water heating in Dutch residential stock, *Energy Build.* 41 (2009) 1223–1232, <http://dx.doi.org/10.1016/j.enbuild.2009.07.002>.
- [37] A.A. Balogun, T.E. Morakinyo, O.B. Adegun, Effect of tree-shading on energy demand of two similar buildings, *Energy Build.* 81 (2014) 305–315, <http://dx.doi.org/10.1016/j.enbuild.2014.05.046>.
- [38] L. Shashua-Bar, D. Pearlmutter, E. Erell, The influence of trees and grass on outdoor thermal comfort in a hot-arid environment, *Int. J. Climatol.* 31 (2011) 1498–1506, <http://dx.doi.org/10.1002/joc.2177>.
- [39] H. Akbari, Shade trees reduce building energy use and CO₂ emissions from power plants, *Environ. Pollut.* 116 (2002) S119–S126, [http://dx.doi.org/10.1016/S0269-7491\(01\)00264-0](http://dx.doi.org/10.1016/S0269-7491(01)00264-0).
- [40] V. Cheng, E. Ng, Thermal comfort in urban open spaces for Hong Kong, *Archit. Sci. Rev.* 49 (2006) 236–242, <http://dx.doi.org/10.3763/asre.2006.4932>.
- [41] F. Kong, C. Sun, F. Liu, H. Yin, F. Jiang, Y. Pu, G. Cavan, C. Skelhorn, A. Middel, I. Dronova, Energy saving potential of fragmented green spaces due to their temperature regulating ecosystem services in the summer, *Appl. Energy* 183 (2016) 1428–1440, <http://dx.doi.org/10.1016/j.apenergy.2016.09.070>.
- [42] M.A. Rahman, A. Moser, T.R.Ötzer, S. Pauleit, Within Canopy Temperature Differences and Cooling Ability of Tilia Cordata Trees Grown in Urban Conditions vol. 114, (2017), pp. 118–128, <http://dx.doi.org/10.1016/j.buildenv.2016.12.013>.
- [43] T.E. Morakinyo, K.W.D.K.C. Dahanayake, E. Ng, Temperature and cooling demand reduction by green-roof types in different climates and urban densities: a co-simulation parametric study, *Energy Build.* 145 (2017) 226–237, <http://dx.doi.org/10.1016/j.enbuild.2017.03.066>.
- [44] M. Foustalieraki, M.N. Assimakopoulos, M. Santamouris, H. Pangalou, Energy performance of a medium scale green roof system installed on a commercial building using numerical and experimental data recorded during the cold period of the year, *Energy Build.* (2016), <http://dx.doi.org/10.1016/j.enbuild.2016.10.056>.
- [45] C.M. Silva, M.G. Gomes, M. Silva, Green roofs energy performance in Mediterranean climate, *Energy Build.* 116 (2016) 318–325, <http://dx.doi.org/10.1016/j.enbuild.2016.01.012>.
- [46] I. Susorova, M. Angulo, P. Bahrami, Brent Stephens, a model of vegetated exterior facades for evaluation of wall thermal performance, *Build. Environ.* 67 (2013) 1–13, <http://dx.doi.org/10.1016/j.buildenv.2013.04.027>.
- [47] K.W.D. Kalani, C. Dahanayake, C.L. Chow, Studying the potential of energy saving through vertical greenery systems: using energypus simulation program, *Energy Build.* 138 (2016) 47–59, <http://dx.doi.org/10.1016/j.enbuild.2016.12.002>.
- [48] H. Yin, F. Kong, A. Middel, I. Dronova, H. Xu, P. James, Cooling effect of direct green façades during hot summer days: an observational study in Nanjing, China using TIR and 3DPC data, *Build. Environ.* 116 (2017) 195–206, <http://dx.doi.org/10.1016/j.buildenv.2017.02.020>.
- [49] C. Yang, X. He, L. Yu, J. Yang, F. Yan, K. Bu, L. Chang, S. Zhang, The cooling effect of urban parks and its monthly variations in a snow climate city, *Remote Sens.* (2017), <http://dx.doi.org/10.3390/rs9101066>.
- [50] X. Xu, S. Sun, W. Liu, E.H. García, L. He, Q. Cai, S. Xu, J. Wang, J. Zhu, The cooling and energy saving effect of landscape design parameters of urban park in summer: a case of Beijing, China, *Energy Build.* 149 (2017) 91–100, <http://dx.doi.org/10.1016/j.enbuild.2017.05.052>.
- [51] B. Zhang, G. di Xie, J. xi Gao, Y. Yang, The cooling effect of urban green spaces as a contribution to energy-saving and emission-reduction: a case study in Beijing, China, *Build. Environ.* 76 (2014) 37–43, <http://dx.doi.org/10.1016/j.buildenv.2014.03.003>.
- [52] R. Berry, S.J. Livesley, L. Aye, Tree canopy shade impacts on solar irradiance received by building walls and their surface temperature, *Build. Environ.* 69 (2013) 91–100, <http://dx.doi.org/10.1016/j.buildenv.2013.07.009>.
- [53] M. Fahmy, S. Sharples, M. Yahya, LAI based trees selection for mid latitude urban developments: a microclimatic study in Cairo, Egypt, *Build. Environ.* 45 (2010) 345–357, <http://dx.doi.org/10.1016/j.buildenv.2009.06.014>.
- [54] L. Chen, E. Ng, X. An, C. Ren, M. Lee, U. Wang, Z. He, Sky view factor analysis of street canyons and its implications for daytime intra-urban air temperature differentials in high-rise, high-density urban areas of Hong Kong: a GIS-based simulation approach, *Int. J. Climatol.* 32 (2012) 121–136, <http://dx.doi.org/10.1002/joc.2243>.
- [55] HKO, *Hong Kong in a Warming World*, (2016).
- [56] Z. Tan, K.K.-L. Lau, E. Ng, Urban tree design approaches for mitigating daytime urban heat island effects in a high-density urban environment, *Energy Build.*

- (2015), <http://dx.doi.org/10.1016/j.enbuild.2015.06.031>.
- [57] M. Bruse, H. Fleer, Simulating surface-plant-air interactions inside urban environments with a three dimensional numerical model, *Environ. Model. Softw.* 13 (1998) 373–384, [http://dx.doi.org/10.1016/S1364-8152\(98\)00042-5](http://dx.doi.org/10.1016/S1364-8152(98)00042-5).
- [58] S. Huttner, M. Bruse, Numerical modeling of the urban climate - a preview on ENVI-MET 4.0, *Seventh Int. Conf. Urban Clim.* (2009) 1–4.
- [59] E. Ng, L. Chen, Y. Wang, C. Yuan, A study on the cooling effects of greening in a high-density city: an experience from Hong Kong, *Build. Environ.* 47 (2012) 256–271, <http://dx.doi.org/10.1016/j.buildenv.2011.07.014>.
- [60] A. Thimonier, I. Sedivy, P. Schleppe, Estimating leaf area index in different types of mature forest stands in Switzerland: a comparison of methods, *Eur. J. For. Res.* 129 (2010) 543–562, <http://dx.doi.org/10.1007/s10342-009-0353-8>.
- [61] J.B. Miller, A formula for average foliage density, *Aust. J. Bot.* 15 (1967) 141–144.
- [62] C. Skelhorn, S. Lindley, G. Levermore, The impact of vegetation types on air and surface temperatures in a temperate city: a fine scale assessment in Manchester, UK, *Landsc. Urban Plann.* 121 (2014) 129–140, <http://dx.doi.org/10.1016/j.landurbplan.2013.09.012>.
- [63] H. Zhang, C.Y. Jim, Contributions of landscape trees in public housing estates to urban biodiversity in Hong Kong, *Urban For. Urban Green.* 13 (2014) 272–284, <http://dx.doi.org/10.1016/j.ufug.2013.12.009>.
- [64] T.E. Morakinyo, L. Kong, K.K.-L. Lau, C. Yuan, E. Ng, A study on the impact of shadow-cast and tree species on in-canyon and neighborhood's thermal comfort, *Build. Environ.* 115 (2017) 1–17, <http://dx.doi.org/10.1016/j.buildenv.2017.01.005>.
- [65] B. Jänicke, F. Meier, M. Hoelscher, D. Scherer, Evaluating the Effects of Façade Greening on Human Bioclimate in a Complex Urban Environment vol. 2015, (2015).
- [66] P. Höppe, The physiological equivalent temperature - a universal index for the biometeorological assessment of the thermal environment, *Int. J. Biometeorol.* 43 (1999) 71–75, <http://dx.doi.org/10.1007/s004840050118>.
- [67] VDI, *Methods for the Human-biometeorological Assessment of Climate and Air Quality for Urban and Regional Planning, Part 1: Climate, VDI Guideline 3787, Part 2. Verein Deutscher Ingenieure* (1998).
- [68] M. Srivani, K. Hokao, Evaluating the cooling effects of greening for improving the outdoor thermal environment at an institutional campus in the summer, *Build. Environ.* 66 (2013) 158–172, <http://dx.doi.org/10.1016/j.buildenv.2013.04.012>.
- [69] U. Berardi, The outdoor microclimate benefits and energy saving resulting from green roofs retrofits, *Energy Build.* 121 (2016) 217–229, <http://dx.doi.org/10.1016/j.enbuild.2016.03.021>.
- [70] H. Lee, H. Mayer, L. Chen, Contribution of trees and grasslands to the mitigation of human heat stress in a residential district of Freiburg, Southwest Germany, *Landsc. Urban Plann.* 148 (2016) 37–50, <http://dx.doi.org/10.1016/j.landurbplan.2015.12.004>.
- [71] J.A. Acero, K. Herranz-Pascual, A comparison of thermal comfort conditions in four urban spaces by means of measurements and modelling techniques, *Build. Environ.* 93 (2015) 245–257, <http://dx.doi.org/10.1016/j.buildenv.2015.06.028>.
- [72] H. Sugawara, S. Shimizu, S. Hagiwara, K. Narita, T. Mikami, How much does urban green cool town? *J. Heat Isl. Inst. Int.* 9 (2014) 11–18.
- [73] B.S. Lin, Y.J. Lin, Cooling effect of shade trees with different characteristics in a subtropical urban park, *HortScience* 45 (2010) 83–86.